JOURNAL OF AIRCRAFT
Vol. 34, No. 3, May–June 1997

# Optimization of an Advanced Business Jet

John W. Gallman*
*NASA Ames Research Center, Moffett Field, California 94035*
and
Randy W. Kaul,† Reuben M. Chandrasekharan,‡ and Michael L. Hinson§
*Learjet, Inc., Wichita, Kansas 67209*

**A new business jet is optimized to fly significantly faster than most current production aircraft while operating from relatively short runways. This new airplane is required to accommodate eight passengers in a double-club arrangement and to carry six passengers for 2800 n mile at a Mach number between 0.81–0.85. Two aircraft optimization codes are used here to ensure the validity of the design results and to identify errors in the analysis methods. These codes include the aircraft analysis methods necessary to evaluate the aircraft performance over an entire mission and optimization routines that enable the development of a family of optimum configurations. The design objective, empty weight, is shown to change approximately 1% between 30–40 deg of wing sweep at a Mach number of 0.81. At a fixed wing sweep of 31.5 deg and a Mach number of 0.81, the empty weight decreases less than 3.5% when the wing's thickness-to-chord ratio is increased from 0.10 to 0.14. A study of the design's sensitivity to Mach number indicated that the optimum empty weight and wing thickness began to change rapidly between the Mach numbers of 0.83–0.85. These optimum sensitivity results enable the selection of a baseline configuration on the basis of both aircraft performance and development risk for the aircraft manufacturer.**

## Nomenclature

| | | |
|---|---|---|
| Alt | = | altitude |
| AR | = | wing aspect ratio, $b_w^2/S_w$ |
| $b$ | = | lifting surface span |
| $C_L$ | = | aircraft lift coefficient |
| $c_l$ | = | airfoil section lift coefficient |
| $I$ | = | load-dependent wing weight |
| $K$ | = | multiplicative constant |
| $n$ | = | aircraft ultimate load factor |
| $q$ | = | flight dynamic pressure |
| $S$ | = | lifting surface planform area |
| $sm$ | = | aircraft static margin |
| $T$ | = | maximum takeoff thrust at 0.7 times the liftoff speed |
| $t/c$ | = | wing thickness-to-chord ratio |
| $V$ | = | aircraft speed, kn |
| $W$ | = | aircraft or fuel weight |
| $\Lambda$ | = | wing sweep |
| $\lambda$ | = | wing taper ratio |
| $\sigma$ | = | atmospheric density ratio, $\rho/\rho_0$ |

*Subscripts*

| | | |
|---|---|---|
| app | = | aircraft approach speed |
| av | = | chord weighted average for $t/c$ |
| $c/4$ | = | quarter chord line |
| empty | = | aircraft empty weight |
| fuel | = | scale factor for cruise fuel weight |
| max | = | maximum airfoil or aircraft lift coefficient |
| op | = | wing outer panel |
| $r$ | = | wing root |
| scl | = | scale factor for wing weight |
| $t$ | = | wing tip |
| TO | = | takeoff configuration |
| $w$ | = | wing |
| wingfuel | = | wing fuel weight |
| ZFW | = | aircraft zero fuel weight |
| $\gamma$ | = | elastic axis |

## Introduction

AS the technology for high subsonic flight has matured, many business jet manufacturers have started developing faster aircraft with significant increases in range. The challenging tradeoff for the business jet designer is to produce a very high-performance airplane with a premium on passenger comfort at a low price. Until quite recently this compromise has resulted in business jets that are slower than the larger commercial transports. The goal of this study is to apply modern transport aircraft technology and optimization tools to the conceptual design of an advanced business jet.

This design study focuses on a Mach 0.81–0.85 business jet that carries six passengers for 2800 n mile. Figure 1 shows the general concept for this new airplane and the accommodation of eight passengers in a fuselage that is a stretch of the Learjet Model 60, a growth version of the Learjet Model 55.[1] Additional design requirements include takeoff from a balanced runway length of 5000 ft, landing at 85% of the maximum takeoff weight on a 3000-ft dry runway (a factored landing distance of 5000 ft), cruise altitudes between 43,000–51,000 ft, and a climb rate of 100 ft/min at 51,000 ft. In comparison, the Learjet Model 60 has a balanced field length of 5360 ft, a landing distance of 3450, and a maximum operating Mach number of 0.81. Because this new aircraft cruises faster than the Model 60 by 0.03–0.07 in Mach number and lands on a 10% shorter runway, a new wing and tail, rather than an evolutionary tweak of the Model 60, are required to satisfy these design specifications. The challenge in this study is to satisfy these performance constraints without significant increases in

Presented as Paper 94-4303 at the AIAA/USAF/NASA/ISSMO 5th Symposium on Multidisciplinary Analysis and Optimization, Panama City Beach, FL, Sept. 7–9, 1994; received Aug. 6, 1995; revision received Feb. 1, 1997; accepted for publication Feb. 17, 1997. 

*Aerospace Engineer, High Speed Aerodynamics Branch; currently Manager, Preliminary Design, Raytheon Aircraft. Member AIAA.
†Senior Engineer, Applied Aerodynamics. Member AIAA.
‡Group Engineer, Applied Aerodynamics. Member AIAA.
§Chief of Aerodynamics. Member AIAA.

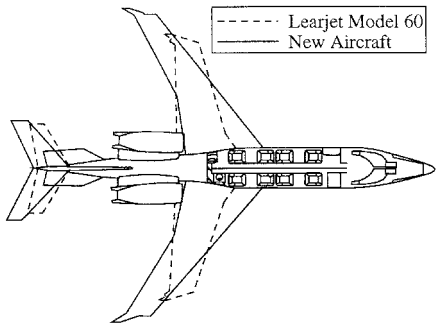


**Fig. 1 Baseline configuration ($S_w$ = 396, $\Lambda$ = 35 deg, $W_{TO}$ = 27,205 lb) and Learjet Model 60 ($S_w$ = 265, $\Lambda$ = 13 deg, $W_{TO}$ = 22,750 lb) with double-club seating layout.**

aircraft purchase price and with minimal risk to the aircraft manufacturer.

Nearly all analysis methods available for conceptual design rely heavily on empirical data from similar aircraft or on simplifying assumptions. In many cases these simplifying assumptions force the designer to ignore a critical issue until a more detailed design phase. In effect, the analysis methods assume a level of performance equal to or greater than current production aircraft. The development effort required in the preliminary and detailed design phases to obtain this assumed level of performance can be interpreted as a measure of risk to the aircraft manufacturer. Risk to the aircraft manufacturer is reduced in this study by verifying the design solutions and performance prediction methods using demonstrated characteristics of current production aircraft.

The approach taken in this study is to design a family of airplanes with cruise speeds of Mach = 0.81, 0.83, and 0.85. This family of airplanes will describe the sensitivity of the optimum design to wing sweep, thickness-to-chord ratio, and Mach number, and will enable the aircraft manufacturer to make design decisions based on both aircraft performance and development risk. Two aircraft optimization codes are used here to ensure the validity of the optimization results. Drastic differences in the optimum configuration or in the performance estimates can indicate an error in an analysis method or the optimization algorithm.

This paper describes the application of aircraft synthesis and numerical optimization software to the design of a new business jet. The analysis methods in two different aircraft synthesis codes are modified to improve the accuracy of performance estimates and validated using flight test data for a Learjet Model 55 aircraft. As part of this validation, the sensitivity of the analysis methods to wing sweep and thickness is considered both as a qualitative check on the validity of the methods and as a way of understanding the design tradeoffs. The relative importance of operational costs and aircraft purchase price is studied by optimizing a series of airplanes with different objective functions. Optimization is also used in this study to define a trapezoidal wing and to determine the sensitivity of this wing design to sweep and thickness. This paper includes a description of the analysis methods used in both synthesis codes, the validation of analysis results with flight test data, the selection of a meaningful objective function, and a comparison of the empty weight of a family of optimum designs.

## Aircraft Analysis Methods

Aircraft optimization can be computationally intensive. Consequently, both aircraft synthesis codes use simple analysis methods that rely on experimental data from similar aircraft. Analysis modules in both codes are used to estimate aerodynamic forces for multiple flight conditions, to predict aircraft weight by adding up estimates for aircraft components and systems, to estimate engine thrust and fuel burn, and to calculate aircraft performance parameters such as range, takeoff field length, landing field length, second segment climb gradient, takeoff rotation, and climb gradient at maximum operating altitude. Many of the methods used for these calculations are similar to those described in Refs. 2 and 3. However, the statistical correlation parameters used to define the weight estimation and runway field length methods have been modified to improve their accuracy for business jet aircraft. The analysis methods used for drag, weight, and maximum lift coefficient are described in detail because they have a direct influence on the optimization results of this study.

### Aerodynamic Modeling

One important difference between the two synthesis codes is the sophistication of the aerodynamic modeling. SPARROW calculates aerodynamic forces using a discrete vortex Weissenger method. This method solves the Prandtl–Glauert equation and calculates induced drag using Trefftz–plane integration. An entire aircraft model (see Fig. 2) was used to represent the downwash on the tail, and hence, the tail's contribution to the pitching moment and static margin. Figure 2 shows that the aerodynamic modeling is sophisticated enough to represent changes in the wing's lift distribution caused by flap deflection and changes in the tail's lift distribution caused by elevator deflection. The computational time required to solve for the 75–100 vortex strengths shown in Fig. 2 is reduced by representing the aerodynamic forces at many different flight conditions as a linear combination of four solutions to the vortex–lattice problem.[4]

The primary aerodynamics module in ACSYNT-L, AEROX,[5] relies on an input aircraft efficiency factor and an approximation of the downwash created at the tail by the wing instead of calculating a load distribution and the mutual interference of lifting surfaces. Similar approximations are used to calculate pitching moment, trim drag, and static stability. Unfortunately, ACSYNT-L cannot consider a constraint on static margin during aircraft optimization. However, AEROX uses a great deal of experimental data and semiempirical relationships to produce accurate performance estimates.

Several modifications to the aerodynamics modules in ACSYNT-L satisfy the requirements of Learjet aircraft. These enhancements include predictions of the influence of winglets on aerodynamic forces and weight, estimates of drag divergence Mach number using the methods of Bayan and Shevell,[6] user-defined drag rise curves, a modification to the calculation of friction drag to account for a specified percentage of laminar flow, and estimates of maximum lift coefficient that are calculated by scaling an input value for aircraft maximum lift coefficient by the cosine of the wing sweep angle. Modifications to the geometric modeling provide for integration of the

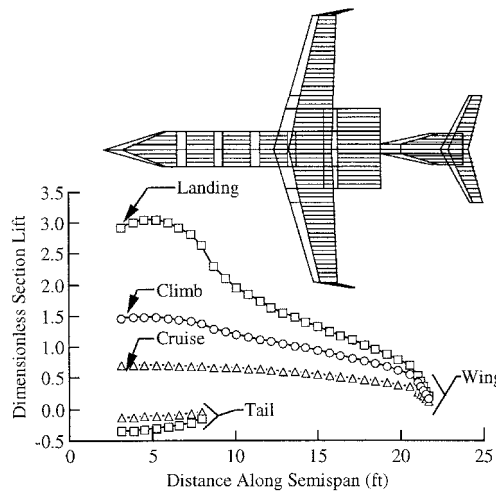


**Fig. 2 Vortex–lattice model of typical business jet.**

winglet with the wing as well as corrections to the wing wetted area to account for the wing–body fairing. Additional analysis modules estimate the aircraft climb rate at cruise altitude and the aircraft landing field length.

### Drag

Drag calculations in SPARROW are divided into three major categories: 1) vortex-induced drag, 2) viscous drag, and 3) compressibility drag. The vortex drag is calculated using the vortex–lattice method at a Mach number of 0.5 for trimmed flight in both cruise and climb. Since the entire aircraft and its wake are modeled, this vortex drag includes trim drag and inviscid interference drag. Lift-dependent viscous drag is assumed to vary parabolically with lift for each airfoil section ($0.003c_l^2$). This relationship represents the variation in minimum section drag with design lift coefficient and assumes the airfoils are cambered for best cruise performance. Section drag values calculated from the corresponding section lift are integrated over the wing span and the tail span to obtain the total lift-dependent viscous drag for the lifting system. An empirical relationship based on flight test data accounted for all other contributions, which are primarily caused by viscous interference, to lift-dependent viscous drag. Viscous drag that is independent of lift is calculated using exposed wetted areas and the von Kármán formulas for the skin friction drag of a flat plate.[7] Corrections are made to these drag calculations to account for surface roughness.[2] Other viscous drag items such as control surface gap drag and nacelle base drag are also treated explicitly. The compressibility drag is defined here as all of the drag caused by an increase in Mach number above 0.5. To estimate this drag increment the local Mach number at the point where the airfoil's upper surface is tangent to the freestream is estimated as a function of airfoil thickness-to-chord ratio, lift coefficient, wing sweep, and freestream Mach number. This local, or crest critical Mach number, is then used to estimate compressibility drag from an average empirical drag rise curve.[8]

Although the drag buildup developed for ACSYNT-L is similar there are a few key differences in the lift-dependent drag and in the compressibility drag. The basic vortex drag is evaluated for the wing, the tail, the body, and the winglets using assumed load distributions, corrections for the mutual interference of lifting surfaces, and an input airplane efficiency factor. Although this type of model can be tuned to provide good performance estimates for a particular class of airplanes it is not capable of capturing the sensitivity of the airplane efficiency factor to a variation in wing sweep. A variation in wing sweep requires a different twist and camber distribution to satisfy a trim constraint at a fixed level of static stability. Even though a user-defined empirical drag rise curve was used to predict compressibility drag in ACSYNT-L, the input drag rise curve used for optimization in both synthesis codes was nearly identical for the range of wing sweeps and thickness-to-chord ratios considered in this study.

### Maximum Lift

Two different methods were used in this study to estimate $C_{L_{\max}}$. The first method scales an input value for aircraft maximum lift coefficient at zero sweep by the cosine of the quarter chord sweep angle

$$C_{L_{\max}} = (C_{L_{\max}})_{\Lambda_{c/4}=0} \cos(\Lambda_{c/4}) \tag{1}$$

Data from similar aircraft[3] suggested that the input value for maximum lift coefficient at zero sweep should be 2.02 for 20 deg of flap deflection and 2.30 for 50 deg of flap deflection. The second method was developed from a critical section theory that assumes the wing stalls when any streamwise airfoil section reaches an empirically determined maximum value. The relationship

$$C_{L_{\max}} = (C_{L_{\max}})_{\Lambda_{c/4}=0}(1.0 - 1.567 \cdot 10^{-3}\Lambda_{c/4}) \tag{2}$$

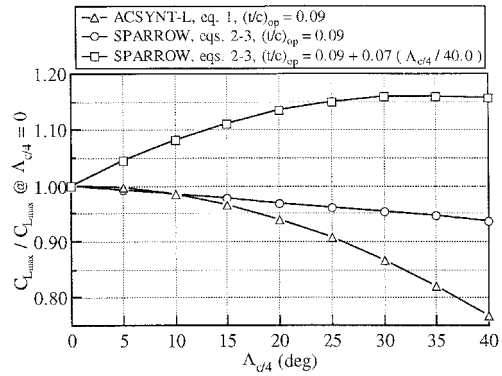


**Fig. 3 Variation in predicted $C_{L_{\max}}$ with wing sweep for clean wing.**

for wing maximum lift[2] was developed by comparing vortex–lattice calculations with experimental data for transport wings with taper ratios of 0.35. For this method, airfoil data available
for DC-9 and DC-10 aircraft were used to estimate the maximum lift at a wing sweep of zero degrees using

$$(C_{L_{\max}})_{\Lambda_{c/4}=0} = 0.9175[0.09 + 21.9(t/c)_{\text{op}} - 74.8(t/c)_{\text{op}}^2] \tag{3}$$

The aircraft's maximum lift is then evaluated by including the tail loads required to trim. Increments in this basic value[9] account for flap and slat deflection.

The experimental data required for accurate estimates of maximum lift are currently unavailable in the published literature, particularly for modern supercritical wings. References 3 and 9 suggest that the maximum lift coefficient decreases with the quarter chord sweep angle; whereas Ref. 10 suggests that a much smaller reduction in maximum lift coefficient with wing sweep can be obtained using wing fences and vortilons. These fences and vortilons enable a streamwise section of a swept wing to obtain the maximum lift coefficient of an unswept airfoil. Figure 3 shows the variation of $C_{L_{\max}}/(C_{L_{\max}})_{\Lambda_{c/4}=0}$ for both maximum lift methods. The results from the second method [Eqs. (2) and (3)] depend on a streamwise section obtaining a zero sweep maximum lift coefficient. A much larger decrease in $C_{L_{\max}}$ is shown in Fig. 3 for Eq. (1) because this method assumes that the spanwise flow along the wing decreases a streamwise section's maximum lift coefficient. The curve designated by the squares in Fig. 3 show that Eq. (3) causes an increase in maximum lift with increasing sweep when the thickness-to-chord ratio is allowed to vary linearly from 0.09 to 0.16 for the variation in sweep between 0–40 deg. Any increase in maximum lift coefficient will lead to optimum aircraft with smaller, lighter wings and will increase the development risk if the result depends on aerodynamic fixes to satisfy a specified field length requirement.

## Weight

The aircraft empty weight is represented as a sum of aircraft component weights in both synthesis codes. However, the fuselage, systems, and engine weights were known or assumed as part of the design specifications, leaving the wing as the only significant weight item that could be influenced by the design variables. Both synthesis codes use relationships between lifting-surface geometry, simple loading parameters, and wing weight that are based on statistical fits to the wing weights of current production aircraft. SPARROW uses the method described in Ref. 11

$$W_w = (1.64I_w + 4.22)S_w \tag{4}$$

where

$$I_w = \frac{nb_w^3\sqrt{W_{\text{TO}}W_{\text{ZFW}}}(1 + 2\lambda)}{(t/c)_{\text{av}}\cos^2(\Lambda_{\text{EA}})S_w^2(1 + \lambda)} \times 10^{-6} \tag{5}$$

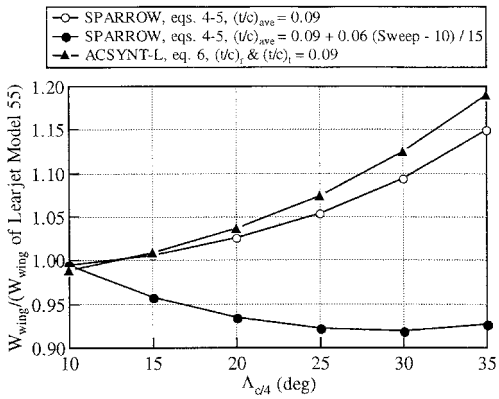


**Fig. 4 Sensitivity of estimated wing weight with respect to wing sweep.**

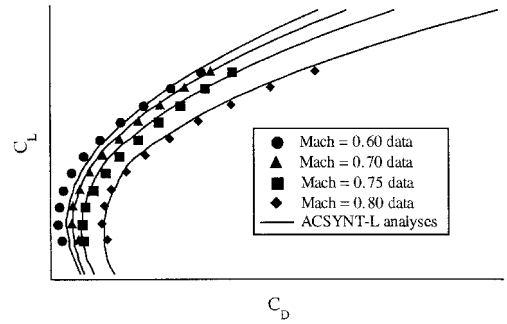


**Fig. 5 ACSYNT-L predictions and flight test drag polars for the Learjet Model 55.**

represents the relationship between the applied loads, the geometric shape, and the load-dependent wing weight. As reported in Refs. 4 and 12, SPARROW also has the capability to design a minimum weight skin-stringer wing structure and use the weight of this structure as a replacement for the parameter $I_w$ in a statistical weight equation similar to Eq. (4). However, Eq. (4) was considered adequate since the new business jet has a cantilever wing structure similar to those used to develop Eqs. (4) and (5) in Ref. 11. The method of Ref. 13 used in ACSYNT-L is given by

$$W_w = K_{scl}\left\{0.0202\left[\frac{W_{TO}nAR}{(1+\lambda)}\right]^{0.5}(S_w)^{0.7} \times \left[\frac{5(2W_{TO}-W_{wingfuel})}{2W_{TO}(4(t/c)_r+(t/c)_t)}\right]^{0.4}\frac{1}{\cos(\Lambda_{c/4})}\right\} \quad (6)$$

where $K_{scl} \approx 1$ is used to force the method to reproduce the known wing weight of a Learjet Model 55. Figure 4 shows that both methods predict a similar sensitivity of wing weight with respect to wing sweep with all other parameters constant. This figure also shows the wing weight decreasing with increasing wing sweep when the wing thickness-to-chord ratio is varied linearly to approximate a family of optimum airplanes designed for a Mach number of 0.81. In this case, the weight savings associated with an increase in thickness offsets the increase in weight commonly associated with increasing wing sweep.

## Synthesis Code Validation

The known performance characteristics of the Learjet Model 55 were used to validate the analysis methods in both synthesis codes before any design studies on a new airplane were performed. Once the analysis methods are considered validated for the Learjet Model 55 they are expected to produce equally accurate results for all aircraft in this weight and performance class. The early analyses identified necessary enhancements or modifications to the existing codes, since these codes were originally developed for larger transport airplanes or for fighters. The analysis results for drag, wing weight, cruise performance, and runway field length were examined in detail and will be discussed briefly in this section.

Flight test data, wind-tunnel data, and calculations based on a surface panel code (VSAERO[14,15]) for the Learjet Model 55 were used to assess the accuracy of the drag calculations in each of the synthesis codes. Ideally, one would use the flight test data for Mach numbers less than 0.5 to validate the vortex and viscous drag components. The overall magnitude of the viscous drag and variations in vortex drag with lift coefficient could be assessed without depending on the accuracy of a compressibility drag model. Unfortunately, flight test drag polars were unavailable for Mach numbers less than 0.50. This led to validation of the total drag values produced by each code for lift coefficients and Mach numbers approximately equal their cruise values without verifying the relative components. The wing twist distribution used for the vortex-lattice model of the Learjet Model 55 in SPARROW was adjusted so that the calculated lift distribution agreed with that produced by VSAERO, thereby increasing the confidence in the vortex drag calculations. After using the Mach = 0.60 data to establish the appropriate surface roughness and including the compressibility drag model of Ref. 8, SPARROW reproduced the flight test drag polars within 5% for cruise lift coefficients and Mach numbers. Wind-tunnel data were used to define the input drag rise curve used in ACSYNT-L to analyze the Learjet Model 55. Figure 5 shows the agreement between the ACSYNT-L calculations and the flight test drag polars after some iterative tuning of the input scale factors that influence the surface roughness and the aircraft efficiency factor. Although the overall drag polars produced by both codes agree with the flight test data, there remain some differences in the drag components that may produce variations in the sensitivity of the objective function with respect to the design variables. The viscous drag models produce approximately the same value for lift-independent drag, but the input drag rise curve used in ACSYNT-L for this analysis produces a more gradual increase in the compressibility drag that starts at a lower Mach number. For the same total drag, this increase in compressibility drag decreases the allowable vortex drag. Fortunately, plans for an increase in airfoil technology forced the use of empirical drag rise curves in both synthesis codes that were nearly identical for the range of wing sweeps and thickness-to-chord ratios considered in the optimization study. The remaining difference in the vortex drag models had a negligible influence on the final optimum designs.

The range constraint is always active and frequently the most important constraint for aircraft optimization problems that do not include drag explicitly in the objective function. A mission analysis of the Learjet Model 55 was used to check range calculations in both codes. Installed engine data available from the engine manufacturer were used in this validation study and in the optimization of the new airplane. Matching the range of a known airplane with a known value of specific fuel consumption represents an additional check of the analysis modules used for weight and drag. Both aircraft synthesis codes matched the flight profile and fuel burn of the Learjet Model 55 within 2%.

The prediction of takeoff and landing field length can be quite complicated if each segment of the maneuver is analyzed in detail with the appropriate aerodynamic forces generated by high-lift systems in ground effect and the appropriate coefficient of friction for braking or acceleration. Typically, the functional form of the equations that represent the required field length are used to correlate the field length performance of similar aircraft. Reference 2 shows that the takeoff field length is proportional to $W_{TO}^2/(\sigma S_w C_{L_{max}} T)$ and that the landing field length is proportional to the square of the stalling speed

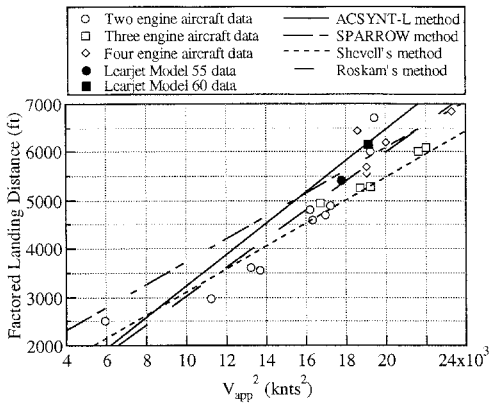


**Fig. 6 Landing field length methods and aircraft data.[2,16]**

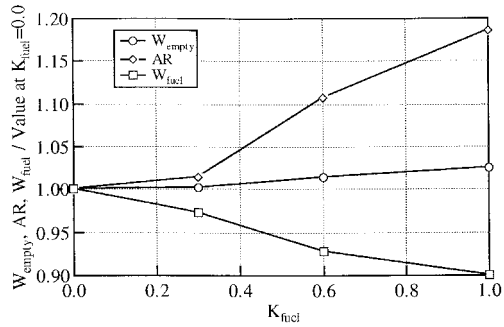


**Fig. 7 Selection of the importance of fuel in the objective function.**

in landing configuration. Both synthesis codes used linear fits to the takeoff and landing field lengths of current production aircraft. The methods used in ACSYNT-L were created by adjusting the constants of proportionality given in Ref. 16 to reduce the error in the prediction of field length performance for Learjet aircraft. Figure 6 shows the landing field length methods used in ACSYNT-L, the method of Ref. 16, and some landing field length data for current production aircraft. This figure also shows how the method of Ref. 2 was modified to produce landing field length estimates for Learjet aircraft in SPARROW. The larger increase in landing field length with increasing approach speed shown for the ACSYNT-L method causes its landing field length estimate to be more sensitive to maximum lift coefficient.

## Optimization

Both aircraft synthesis codes used in this study were configured to minimize the empty weight of an aircraft that transports six passengers in a double-club seating arrangement for a distance of 2800 n mile at cruise Mach numbers of 0.81, 0.83, and 0.85. For weight estimation only an additional 400-lb payload was used to provide a margin on ramp weight. These aircraft were required 1) to takeoff from a balanced runway length of 5000 ft, 2) to climb to an initial cruising altitude of 43,000 ft, 3) to maintain a climb rate of 100 ft/min at 51,000 ft, 4) to land at 85% of the maximum takeoff weight in less than a factored landing distance of 5000 ft, 5) to maintain a cruise thrust that is greater than the cruise drag, 6) to have sufficient wing fuel volume with 5661 lb of fuselage fuel, and 7) to be trimmed during all phases of flight. In addition to this basic set of constraints, SPARROW required the candidate designs 1) to have a specified static margin based on a reference chord of 6.73 ft, 2) to maintain a climb gradient of 2.4% with an engine-out just after takeoff, and 3) to carry zero lift on the pylons and ventral fins at the cruise condition. ACSYNT-L used wing area, wing aspect ratio, wing sweep, a scale factor on wing thickness, and the Mach number for the top-of-climb constraint as design variables. In SPARROW, wing area, wing span, wing sweep, average wing thickness-to-chord ratio, the Mach number for the rate of climb constraint, the longitudinal location of the wing, the tail area, eight lifting surface incidence values, takeoff flap deflection, cruise altitude, takeoff weight, and zero fuel weight were used to determine the optimum business jet.

SPARROW used the optimization routine NPSOL to minimize empty weight subject to 12 nonlinear constraints and both upper and lower bounds on each of the 19 design variables. NPSOL, a gradient-based optimizer, uses a sequential quadratic programming algorithm to solve the design problem. This algorithm solves a quadratic subproblem to determine the appropriate search direction in design space, performs a line search in this direction, and minimizes an augmented Lagrangian merit function.[17] The finite difference option in NPSOL was used to approximate gradients and an attempt was made to have variable, function, and first derivative values of order 1.0, where 1.0 is interpreted to within a couple orders of magnitude. The linear scaling used for both design variables and constraints represents a compromise between keeping both variable and function values of order 1.0 and obtaining first derivative values that are nearly equal for all of the functions in the scaled design space. Constraint violations, the step length used for the current line search through design space, and the value of the projected gradient are monitored to ensure convergence to the Kuhn–Tucker conditions for optimality.[18] For all the SPARROW optimization results, the aircraft empty weight and the active constraint values varied less than 0.001% during the last few iterations.

ACSYNT-L used CONMIN[19] to solve an aircraft optimization problem defined by five design variables and six nonlinear constraints. All of the design variables were unbounded throughout the optimization, except wing tip thickness-to-chord ratio, which had a lower bound of 0.08 included as one of the nonlinear constraints. CONMIN, a gradient-based optimizer, uses the methods of feasible directions[20] to determine the appropriate search direction in design space and performs a line search in this direction that minimizes the design objective. Finite difference calculations are used to evaluate the gradients of the objective function and all explicit constraints. Constraints on range, minimum cruise altitude, and trim are all satisfied iteratively within the ACSYNT-L analysis routines. For all of the designs presented in this study, the constraint violations were forced to be less than 0.4% and the objective function was forced to vary less than 0.05% over three iterations.

Several different objective functions of the form $W_{empty} + K_{fuel}W_{fuel}$ were considered by comparing the empty weight, aspect ratio, and required cruise fuel $W_{fuel}$ of a series of optimum airplanes. Figure 7 shows the optimization results for values of $K_{fuel}$ between 0.0–1.0, where approximately 40% of the objective function value is attributed to fuel weight when $K_{fuel}$ = 1.0. This figure shows that a 10% reduction in cruise fuel can be obtained with an 18% increase in wing aspect ratio and a 2.5% increase in empty weight. This tradeoff between cruise fuel and empty weight represents a tradeoff between aircraft purchase price and operational cost because purchase price is approximately proportional to aircraft empty weight.

Even though a 2.5% increase in aircraft purchase price seems small, aircraft empty weight is used as the objective function in this study for the following reasons. Most companies replace their business jets every 10 years or when the latest model has a significant increase in performance or comfort. Since most of these jets accumulate approximately 500 h per year with relatively short trips (1–2 h), the 10% savings in cruise fuel will be worth less than half the 2.5% increase in purchase price required to achieve it.

## Results

All of the aircraft considered in this study were assumed to have winglets with an aspect ratio of 2.33, a taper ratio of

0.35, and a root chord equal to 65% of the wing tip chord. These aircraft were also assumed to have a high-lift system that consists of double-slotted flaps. Experience with winglets on other Learjet aircraft suggests that a significant savings in induced drag can be obtained for the cost of the winglet weight. Designing wings without slats avoids some high-lift system complexity and produces a conservative optimum wing area.

The optimization results presented here, for aircraft with minimum empty weight, have range, landing field length, climb rate at 51,000 ft, minimum cruise altitude, and cruise trim as active constraints. Results obtained using SPARROW also include static margin, second segment climb gradient, zero pylon lift, and zero ventral fin lift as active constraints. All of the variables were free from bound constraints, except the thickness-to-chord ratio that was at its lower bound for the ACSYNT-L, Mach = 0.85 design, and the wing sweep that was at its upper bound of 35 deg in all SPARROW designs. Optimization convergence tolerances were approximately the same for all results and within the bounds stated earlier. In most cases, each solution presented was checked by restarting the optimization process from a different location in design space.

Preliminary optimization results from the two codes were different by 0.06 in average wing thickness-to-chord ratio, 4 deg in wing sweep, and 19% in gross wing area for an airplane with a cruise Mach number of 0.81. Each of these optimum designs were analyzed in both codes to test validity of the results and as an initial search for programming errors. Figure 8 shows the drag rise characteristics estimated by both codes for both airplanes at Mach = 0.81 and the cruise lift coefficient of 0.40. Both codes agree reasonably well when used to analyze the ACSYNT-L design that has an average wing thickness-to-chord ratio of approximately 0.095. However, 55–60 additional drag counts are predicted by ACSYNT-L for the thicker SPARROW wing ($t/c$ = 0.15). An error in the wing–fuselage interference drag predicted by ACSYNT-L caused this extreme sensitivity to wing thickness. This experience demonstrates the value of applying two aircraft optimization codes to the same problem.

Eliminating this error in ACSYNT-L improved the agreement in the drag predictions, however, the optimization results still showed significant differences in wing thickness, sweep, and area. Table 1 shows these differences and some results that emphasize the influence of the maximum lift on the optimum design. Table 1 shows that the ACSYNT-L results produce a minimum empty weight at 31.5 deg of wing sweep (see column 1) and that the minimum empty weight suggested by SPARROW occurs at 35 deg of sweep (see column 2) with the wing sweep variable at its upper bound. As described earlier, scaling the maximum lift coefficient by the cosine of the wing sweep produces a larger decrease in maximum lift than the method of Eqs. (2) and (3) (see Fig. 3). It is interesting that the increase in wing weight associated with increasing

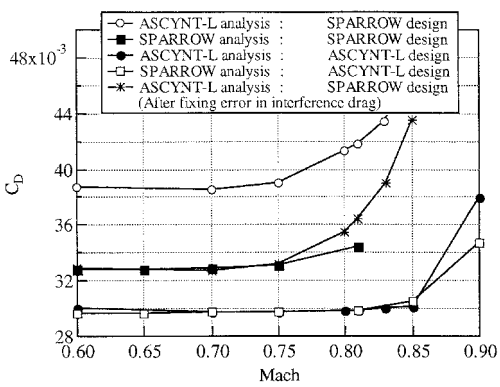


**Fig. 8 Drag rise curves for preliminary optimization results.**

**Table 1 Sensitivity of optimum design results to the $C_{L_{max}}$ model at Mach = 0.81**

| Parameter | ACSYNT-L, Eq. (1) | SPARROW, Eqs. (2) and (3) | SPARROW, Eq. (1) |
|---|---|---|---|
| $S_w$ | 382.0 | 314.0 | 393.0 |
| AR | 6.75 | 6.00 | 6.03 |
| $(t/c)_{av}$ | 0.105 | 0.15 | 0.13 |
| $\Lambda_{c/4}$ | 31.5 | 35.0 | 29.0 |
| Alt | 47,359 | 45,864 | 46,203 |
| $sm$ | NA | 0.2 | 0.2 |
| $W_{TO}$ | 26,950 | 25,823 | 27,112 |
| $W_{empty}$ | 16,114.0 | 15,361.0 | 16,319.0 |

sweep is too small to force SPARROW to suggest an optimum wing sweep of less than 35 deg. These differences in wing sweep also lead to differences in the optimum wing thickness-to-chord ratio. The ACSYNT-L result suggests that an average wing thickness-to-chord ratio equal to 0.105 is optimum, whereas SPARROW suggests that 0.15 is optimum. The smaller value of thickness-to-chord ratio in the ACSYNT-L model causes an increase in wing weight, which also contributes to the need for a larger wing to satisfy the landing field length constraint. The increase in induced drag associated with increasing aircraft weight begins to offset some of the reductions in compressibility drag as the wing sweep increases from 30 to 35 deg in both synthesis codes. Column 3 of Table 1 shows that, when the maximum lift coefficient is scaled by the cosine of the wing sweep [Eq. (1)], SPARROW produces an optimum wing sweep of 29 deg and a thickness-to-chord ratio of 0.13. Using Eqs. (2) and (3) instead of Eq. (1) to estimate the $C_{L_{max}}$ in landing configuration produces a 20% increase in $C_{L_{max}}$ at 35 deg of wing sweep. The results of columns 2 and 3 also show that this 20% increment in $C_{L_{max}}$ reduces the aircraft empty weight by 6% and the wing area by 20%. These results identify maximum lift as a critical design issue for this airplane.

A study of the sensitivity of the Mach = 0.81 design to wing sweep and thickness was used to gain a better understanding of the design space and to explain why the two codes continued to give different values for optimum wing thickness. The SPARROW results obtained for this sensitivity study were obtained using a required static margin of 0.4 because this corresponded to the longitudinal wing locations used for the ACSYNT-L designs. Unfortunately, ACSYNT-L could not consider static margin as a constraint in the optimization. Figure 9 shows the variation in aircraft empty weight with parametric variations in both wing sweep and average wing thickness-to-chord ratio. These results were generated by fixing the value of wing sweep or thickness and determining the optimum values for the remaining design variables. Figure 9 shows that when the wing sweep is varied from 30 to 40 deg the variation in empty weight is approximately 1%, which suggests that this design is insensitive to wing sweep. Varying the thickness-to-chord ratio between 0.10–0.14 at a constant wing sweep of 31.5 deg causes the empty weight to decrease by 3.5%. These results indicate that the design space is flat with respect to sweep, but the choice for wing thickness remains a significant issue.

Two SPARROW optimization results that satisfied tolerances on optimality and constraint violation of less than 0.001% provide additional evidence that this design is insensitive to wing sweep. Both of these Mach = 0.81 designs have the same optimum empty weight, but one has a wing sweep of 31.2 deg and a thickness-to-chord ratio of 0.14, whereas the other has a wing sweep of 35 deg and a thickness-to-chord ratio of 0.16. These two designs were created by starting the optimization process from two drastically different locations in design space.

The ACSYNT-L configurations for the Mach numbers of 0.81, 0.83, and 0.85 were analyzed with SPARROW to provide

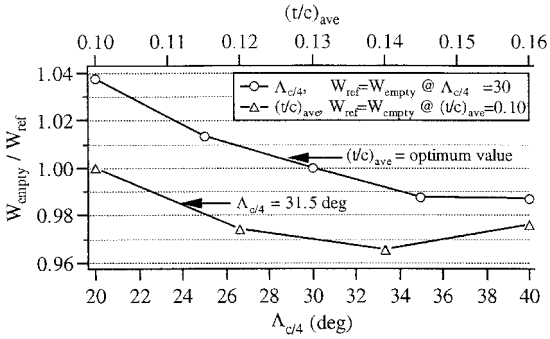


**Fig. 9 Optimum sensitivity of empty weight with respect to wing sweep (SPARROW results).**

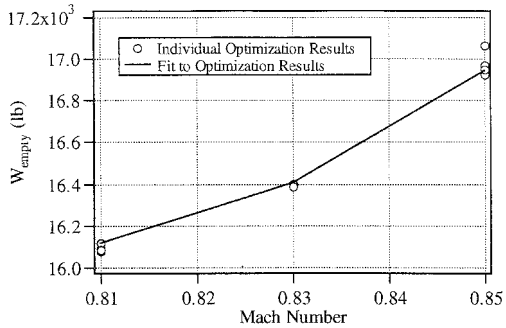


**Fig. 10 Optimum sensitivity of empty weight with respect to Mach number.**

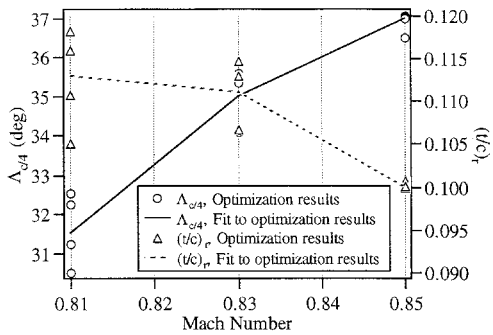


**Fig. 11 Optimum sensitivity of wing sweep and thickness with respect to Mach number.**

an additional check on the validity of these optimization results. Significant violations in the range constraint would indicate an error in the analysis or methods for either weight or drag. These analyses suggested that the Mach 0.81 configuration exceeded its required range by 4%, that the Mach 0.83 configuration missed its required range by 1%, and that the Mach 0.85 configuration missed its required range by 6%. Given the known differences in the analysis methods used for weight and drag, these constraint violations were considered acceptable.

The three Mach numbers considered in this study provide the sensitivity of this design to cruise speed and an indication of the development risk associated with this aircraft. Figure 10 shows that the optimum empty weight predicted by ACSYNT-L increases by 1.8% between Mach 0.81–0.83 and by 3.7% between the Mach numbers of 0.83–0.85. Figure 11 shows the variation in wing sweep and wing thickness-to-chord ratio with Mach number for the same optimization results presented in Fig. 10. The thickness-to-chord ratio remains approximately constant between the Mach numbers of 0.81–0.83, but decreases by about 0.01 to a lower bound at Mach = 0.85. Wing sweep is shown to increase in a nearly linear fashion from 31.5 deg at Mach = 0.81 to 37.0 deg at Mach = 0.85. Each of the data points plotted in Figs. 10 and 11 at the same Mach number represent a different optimization run. The scatter between these points demonstrates that the optimum design is insensitive to wing sweep and thickness and indicates the variation obtained by ACSYNT-L for a convergence tolerance on an empty weight of 0.05%. Figure 10 shows that the empty weight varies less than 1% for all Mach numbers. This variation in empty weight produces a variation in wing thickness-to-chord ratio of 0.023 and a variation of 2 deg in wing sweep at a Mach number of 0.81 (see Fig. 11).

**Table 2 Optimum configurations designed for Mach = 0.83**

| Parameter | ACSYNT-L | SPARROW |
|---|---|---|
| $S_w$ | 396.0 | 416.1 |
| AR | 6.80 | 6.85 |
| $(t/c)_{av}$ | 0.103 | 0.146 |
| $\Lambda_{c/4}$ | 35.0 | 35.0 |
| Alt | 47,500 | 45,135 |
| $sm$ | NA | 0.4 |
| $W_{TO}$ | 27,205.0 | 27,508.7 |
| $W_{empty}$ | 16,404.0 | 16,411.7 |

The selection of a baseline configuration for further development was based on the results of Figs. 10 and 11 and a subjective assessment of development risk. The Mach 0.81 and 0.83 designs shown in Figs. 10 and 11 are quite similar, but the sensitivity of the optimum design to both empty weight and thickness increases between a Mach number of 0.83–0.85. This increase in sensitivity, a wing sweep of 37.0 deg, and a thickness-to-chord ratio variable at its lower bound all represented an increase in development risk. Further analysis of the Mach 0.83 design suggested that it would satisfy the range constraint at a Mach number of 0.85 by using the 400-lb ramp weight margin for additional fuel and by cruising at a lower altitude than was considered in this study. Table 2 shows the design results at Mach = 0.83 produced by both synthesis codes with the same analysis methods for maximum lift. These designs both have a wing sweep of 35.0 deg, wing areas that are approximately equal to 400 ft$^2$, and an empty weight of about 16,400 lb. The ACSYNT-L design was chosen as the baseline configuration for the development of a transonic wind-tunnel model because the reduced thickness represented a lower bound on airfoil technology. The detailed aerodynamic design could then proceed as an opportunity to increase the wing thickness.

## Conclusions

A family of optimum aircraft configurations was developed in this study using two synthesis codes and two optimization routines. The use of two codes enabled the identification of errors in the analysis routines and increased the validity of the optimization results. Synthesis code validation results indicate that range can be estimated within 5% and that factored landing distance can be predicted within 2–300 ft for aircraft that are similar to a Learjet Model 55. Maximum lift was identified as a critical design issue by showing that the optimum empty weight decreases by 6% and the optimum wing area decreases by 20% when the available maximum lift coefficient is increased by 20% at 35 deg of wing sweep. This sensitivity suggests that better methods need to be developed for the prediction of maximum lift during conceptual design. A variety of objective functions that included different proportions of aircraft empty weight and fuel weight were used to show that a 10% savings in cruise fuel could be obtained with an 18% increase in aspect ratio and a 2.5% increase in the weight of an aircraft designed for minimum empty weight. Even though this seems like an equitable tradeoff, aircraft empty weight was used as the objective function for the remainder of the study because of the requirement to keep the aircraft purchase price as low as possible. A parametric variation in wing sweep be-

tween 30–40 deg showed that the optimum empty weight changed approximately 1%. At a fixed wing sweep of 31.5 deg and a Mach number of 0.81, the empty weight decreases less than 3.5% when the wing's thickness-to-chord ratio is increased from 0.10 to 0.14. A study of the design's sensitivity to Mach number indicated that the optimum empty weight and wing thickness began to change rapidly between Mach numbers 0.83–0.85. These optimum sensitivity results enabled the selection of a final configuration on the basis of both aircraft performance and development risk for the aircraft manufacturer. The final configuration selected for the development of a transonic wind-tunnel model has a wing sweep of 35 deg, an average wing thickness-to-chord ratio of 0.10, and a gross wing area of 396 $ft^2$.

## References


[1]Chandrasekharan, R. M., Hawke, V. M., Hinson, M. L., Kennelly, R. A., Jr., and Madson, M. D., "Aerodynamic Tailoring of the Learjet Model 60 Wing," Society of Automotive Engineers, Paper 932534, Sept. 1993.

[2]Shevell, R. S., *Fundamentals of Flight*, Prentice–Hall, Englewood Cliffs, NJ, 1983.

[3]Torenbeek, E., *Synthesis of Subsonic Airplane Design*, Delft Univ. Press and Martinus–Nijhoff Publishers, The Netherlands, 1982.

[4]Gallman, J. W., Kroo, I. M., and Smith, S. C., "Optimization of Joined-Wing Aircraft," *Journal of Aircraft*, Vol. 30, No. 6, 1993, pp. 897–905.

[5]Axelson, J. A., "AEROX-Computer Program for Transonic Aircraft Aerodynamics to High Angles of Attack," NASA TMX 73208, Feb. 1977.

[6]Bayan, F., and Shevell, R., "Development of a Method for Predicting the Drag Divergence Mach Number and the Compressibility Drag Due to Conventional and Supercritical Wings," Dept. of Aeronautics and Astronautics, SUDAAR 522, Stanford Univ., Stanford, CA, July 1980.

[7]Von Kármán, T., "Turbulence and Skin Friction," *Journal of the Aeronautical Sciences*, Vol. 1, No. 1, 1934, pp. 1–20.

[8]McGeer, T., and Shevell, R., "A Method for Estimating the Compressibility Drag of an Airplane," Dept. of Aeronautics and Astronautics, SUDAAR 535, Stanford Univ., Stanford, CA, Jan. 1983.

[9]Hoak, D. E., and Fink, R. D. (eds.), "USAF Stability and Control DATCOM," Wright–Patterson AFB, OH, April 1978.

[10]Furlong, G. C., and McHugh, J. G., "A Summary and Analysis of the Low-Speed Longitudinal Characteristics of Swept Wings at High Reynolds Number," National Advisory Committee for Aeronautics, Rept. 1339, 1957.

[11]Beltramo, M. N., Trapp, D. L., Kimoto, B. W., and Marsh, D. P., "Parametric Study of Transport Aircraft Systems Cost and Weight," NASA, CR 151970, April 1977.

[12]Gallman, J. W., and Kroo, I. M., "Structural Optimization for Joined-Wing Synthesis," *Journal of Aircraft*, Vol. 33, No. 1, 1996, pp. 214–223.

[13]Moore, M., and Samuels, J., "ACSYNT—Aircraft Synthesis Program—User's Manual," NASA Ames Research Center, Moffett Field, CA, Sept. 1990.

[14]Maskew, B., "Program VSAERO, a Computer Program for Calculating the Nonlinear Characteristics of Arbitrary Configurations, Theory Document," NASA CR 4023, Sept. 1987.

[15]Maskew, B., "Program VSAERO, a Computer Program for Calculating the Nonlinear Characteristics of Arbitrary Configurations, Users Manual," NASA, CR 166476, Dec. 1982.

[16]Roskam, J., *Airplane Design—Part I*, Roskam Aviation and Engineering Corp., Ottawa, KS, 1985.

[17]Gill, P. E., Murray, W., and Wright, M. H., *Practical Optimization*, Academic, New York, 1981.

[18]Gill, P. E., Murray, W., Saunders, M. A., and Wright, M. H., "User's Guide for NPSOL (Version 4.0): A Fortran Package for Nonlinear Programming," Dept. of Operations Research, TR SOL 86-2, Stanford Univ., Stanford, CA, Jan. 1986.

[19]Vanderplaats, G. N., "CONMIN-A FORTRAN Program for Constrained Function Minimization—User's Manual," NASA Ames Research Center, TMX 62282, Moffett Field, CA, Aug. 1973.

[20]Vanderplaats, G. N., *Numerical Optimization Techniques for Engineering Design: With Applications*, McGraw–Hill, New York, 1984.